Persulfate activation by swine bone char-derived hierarchical porous carbon: multiple mechanism system for organic pollutant degradation in aqueous

Xuerong Zhou [a], Zhuotong Zeng [b], Guangming Zeng [a,*], Cui Lai [a,*], Rong Xiao [b,*], Shiyu Liu [a], Danlian Huang [a], Lei Qin [a], Xigui Liu [a], Bisheng Li [a], Huan Yi [a], Yukui Fu [a], Ling Li [a], Zhihong Wang [a].

[a] College of Environmental Science and Engineering, Hunan University and Key Laboratory of Environmental Biology and Pollution Control (Hunan University), Ministry of Education, Changsha 410082, PR China.

[b] Department of Dermatology, Second Xiangya Hospital, Central South University, Changsha 410011, PR China.

* Corresponding author at: College of Environmental Science and Engineering, Hunan University, Changsha, Hunan 410082, China. Tel: +86–731–88822754; fax: +86–731–88823701. E-mail address: zgming@hnu.edu.cn (G.M. Zeng) , laicui@hnu.edu.cn (C.Lai) and xiaorong65@csu.edu.cn (R. Xiao)

Abstract

Recent years, application of biochar in catalysis field has attracted increasing attention for it is an effective, inexpensive and environment friendly methods to solve the environmental issues. The aim of this work is to apply bone char (BBC) into persulfate (PS) activation system and achieve efficient 2, 4-dichlorophenol (2, 4-DCP) degradation. This work first applied de-fatted swine bone as the biochar precursor. The as-prepared BBC has considerable high surface area (1024.34 m^2/g) and wide porous distribution. Especially the hierarchical porous structure is supposed to accelerate the electrons transfer in this catalytic process. The results showed that over 85% of 2, 4-DCP can be removed in 30 min and almost 100% of 2, 4-DCP can be completely degraded in 2 h. Further research found that 2, 4-DCP was eliminated by both radical and non-radical pathway, and radical pathway dominated the catalytic process in BBC/PS system. $^{\bullet}OH$, $SO_4^{\bullet-}$, $O_2^{\bullet-}$ and $^1O_2$ all contributed to this system, among which the $^{\bullet}OH$ played the most significant role. Liner Sweep Voltammetry (LSV) and electrochemical impedance spectroscopy (EIS) were taken to verify the non-radical pathway did exist in this system. Owing to the existence of multiple mechanisms, the BBC/PS system remained highly efficient in real surface water and it had remarkable adaptability to various environment conditions. This research commits to proposing a novel strategy for green remediation of contaminated water.

Keywords: Advanced oxidation process; Bone char; Persulfate activation; 2,4-dichlorophenol; Degradation

1. Introduction

As a typical phenolic compound, 2, 4-dichlorphenol (2, 4-DCP) is widely existed in our daily life [1]. It is mainly produced by oil refineries, coal industry and chemical plants. Generally, 2, 4-DCP serves as the precursor of herbicide, and it enters the environment through soil infiltration or wastewater discharge [2]. Besides, it can damage the nervous system and even cause death. Considering its universality and toxicity, 2, 4-DCP, as a refractory pollutant in aquatic environment, needs to be controlled efficiently.

Advanced oxidation processes (AOPs, including photocatalysis [3-8], electrocatalysis [9] and Fenton oxidation [10, 11], ozonation [12], etc.) are recognized as potential approaches to degrade 2, 4-DCP. Sulfate radical ($SO_4^{\bullet-}$) generated from persulfate (PS) activation process is regarded as an efficient one, which has been extensively studied [13]. $SO_4^{\bullet-}$ has a remarkable redox potential (1.8-2.7 versus 1.5-2.8 V NHE of hydroxyl radical) and a long half-lifetime (30-40 μs versus 20 ns of hydroxyl radical) [14], which can degrade organic pollutant into CO_2, H_2O and inorganic salt. Besides, $SO_4^{\bullet-}$ has selective reactivity, it shows a higher reactivity for phenolic compounds, such as 2, 4-DCP [15].

Activator is the key in PS activation system. Typical carbonaceous materials have been applied in PS activation system, which is an economical approach with no need of any external energy supply [16] and avoids the risk of metal leaching [13, 17]. PS has been reported being activated by typical carbon materials such as single-walled carbon nanotubes, graphene and nano diamonds [18]. Previous studies demonstrated that surface area, defect structure and surface functional electron-rich groups are the primary

influencing factors of catalytic effect of carbonaceous materials [19, 20]. Generally, heteroatomic doping (including N, B, O, P, S, etc.) [21, 22] and metal introduction [23] are the common methods to enlarge catalytic regions. Duan's group reported that the doped of nitrogen could accelerate the catalytic rate of reduced graphene oxide from 0.004 min^{-1} to 0.391 min^{-1} [24].Dong's group verified that the methylene blue (MB) degradation climbed from 39% to 99% after 5 wt. % CoO was added into mesoporous carbon nitride materials. Although the carbon nanomaterials mentioned above have been verified to have good catalytic activity, the limited source, complex synthesis process and further environmental risks hinder the further application of these materials.

Biochar is a carbon-rich solid originates from the pyrolysis of biomass, which is regarded as a green carbonaceous material for its simple design and low cost [25, 26]. Recently, biochar has received great concern in the field of environmental catalysis because it has adjustable specific surface area (SSA) and a mass of surface functional groups. Up to now, plants such as bamboo, wood and pine needle derived biochar have been applied as catalyst in PS activation system. Moreover, sludge derived biochar as a catalyst has also been repeatedly reported [27-29]. Whereas, conventional biochar which was employed in PS activation system usually requires modification to achieve expected catalytic effect [30, 31]. Guo and co-workers reported that the removal rate of sulfamethoxazole soared from 23% to 99% when the biochar was decorated by Fe(III) and nitrogen [32]. Nevertheless, the decorating process not only increases the cost and time of materials synthesis but also brings the risk of heavy metal leaching. Hence, it is urgent to find a brand-new and environment friendly raw material of biochar to achieve

efficient activation of PS.

In recent years, bone derived char has gained increasing attention for its special surface character, pore volume, porous size and surface charge distribution. In this study, animal-derived char derived by swine bone was first introduced in PS activation system [33, 34]. Because of the natural structure and composition of bone char (BBC), it was assumed to be effective in PS activation system. Bone obtains nature stable structures at many length scales which can enlarge the SSA of BBC, and it may bring strong adsorption capacity to BBC [35]. It is widely recognized that the adsorption process is important for catalytic system. Furthermore, bones are composed of organic compounds and minerals. The protein and collagen in bone act as carbon precursor and the nature minerals can work as the self-template for BBC. Meanwhile, hydroxyl apatite and calcium phosphate, as the basis of bone, could be the phosphorus doping precursor. On account of the comprehensive influence of natural pore and organic matters pyrolysis, as-prepared bone char could obtain a hierarchical porous structure. Note-worthily, Huang and co-workers have used swine bone as precursor of electrocatalytic electric double-layer capacitors, and they believed that the hierarchical porous structure could accelerate electron transfer [36]. This feature is supposed to be valid in non-radical pathway for PS activation system. In addition, the yield of swine bone is large. Owing to the sustained expanding of China and U.S, global production of pork is predicted to climb 1% to 114.6 million tons in 2019 (USDA, 2018). Moreover, as a by-product of pork, swine bone was generally classified as kitchen waste, and the long-term degradation limited the application of bone in compost. The usage of swine bone is also a kind of way to achieve waste reused. In

summary, BBC is a promising candidate for PS catalysis.

In this research, de-fatted swine bone was the precursor of biochar to realize efficient decomposition of 2, 4-DCP in PS activation system. The objectives of this research were to: i) raise a new strategy to activate PS by BBC and determine the efficiency of this treatment; ii) explore the mechanism of BBC/PS system; iii) investigate the influence factors of this system and apply it to real water.

2. Materials and methods

2.1 Chemicals and synthesis

All chemicals were reagent grade and applied as received. The bone char-derived hierarchical porous carbon was prepared by the pyrolysis of de-fatted swine bone. The spareribs were purchased from a local market (Changsha, China). For simulating the condition of swine bones in kitchen waste, they were dried out after cooking. Cooked bones contain relatively less grease, which is beneficial to avoid the blockage of tuber furnace during pyrolysis process. Collected bones were first carbonized by tuber furnace in the N_2 atmosphere at 450 °C. After grinding, pre-carbonized particles were further carbonized at 900 °C (ramp at 5 °C/min and hold for 2 h). The product was soaked in 150 mL of HNO_3 (6 M) for 12 h, then rinsed with deionized water to neutral and dried at 110 °C for 12 h. The obtained material was labelled as BBC.

2.2 Characterization

The scanning electron microscope (SEM, JSM-6700F) furnished with energy dispersive X-ray spectrometer (EDX) was applied to explore the morphological characteristics and elements distribution of BBC. The SSA, nitrogen adsorption-

desorption isotherm of BBC and other porous properties were measured by Brunauer-Emmett-Teller (BET) gas adsorption isotherm with N_2 gas on Quantachrome Autosorb AS-1. X-ray photoelectron spectroscopy (XPS) and Raman spectra were measured to detect the constituent elements and structure of BBC. The surface functional groups of BBC were performed on a Fourier transform infrared spectrometer (FT-IR).

2.3 Persulfate activation reaction

All batch experiments were carried out in the beaker of the same size at room temperature. For the uniform distribution, shaking rate was keeping at 500 rpm on magnetic stirrers. An hour adsorption was taken to identify the effect of the adsorption process on the abasement of 2, 4-DCP. Specifically, BBC was first dispersed into the 2, 4-DCP (0.2 g/L) solution, and the absorption equilibrium was achieved after 1 h shaking. Secondly, the equally weighted PS (2 g/L) was added into the above solution, and catalytic oxidation started. At each predetermined interval (5, 10, 30, 60 and 120 min), the samples were filtered by 0.45 μm nylon filter and propriety amount of methanol was used to quench the further radical reactions. The amount of PS and BBC was adjusted to find the relatively efficient dosage. The pH of solution was adjusted by 0.1 M HNO_3 or 0.1 M NaOH. NaCl was chosen as the additive of Cl^- to investigate the influence of different Cl^- concentration. After each run, BBC was washed by ultrapure water and ethyl alcohol for 3 times respectively, then dried at 60 °C, the stability tests were achieved by collecting these dried BBC. In order to further explore the role of radical in this system, several radical scavengers were chosen to quench the radical reaction. As it has been reported, both ethanol (EtOH) and tert-butyl-alcohol (TBA) could scavenge $SO_4^{\bullet -}$ and

$^{\cdot}OH$, while benzoquinone (BQ) and NaN_3 were generally employed as scavenger of $O_2^{\cdot-}$ and $^1O_2$ respectively. All measurements were taken in duplicate or triplicate. The variation of each parameter was less than 5%, and the data represented as the mean values.

The reaction was also taken in real water. The surface water samples were collected from Xiangjiang River and Taozi Lake (Changsha, China). The Xiangjiang River is a tributary of the Yangtze River and Taozi Lake is at the foot of Yuelu Mountain.

2.4 Analytical methods

Agilent 1200 high performance liquid chromatography with a C18 column (5.0 μm, 4.6 mm × 250 mm) was applied to measure the concentration of 2,4-DCP. The flow rate of mobile phase was set as 1 mL/min, while methanol and water (60:40, v/v) constituted the mobile phase. The gas chromatography coupled with mass spectrometry (GC-MS) (Shimadzu QP-2010 Ultra instrument with a DB-5 column (30 m x 0.25 nm x 0.25 μm)) was used to analyze the dechlorination process of 2,4-DCP. The temperature ramp was: 40 °C for 2 min, 12 °C/min up to 100 °C, 10 °C/min up to 200 °C, 20 °C/min up to 260 °C and hold time 2 min. The temperature of the inject port, ion source and transfer line was 250, 230 and 280 °C, respectively. The column was heated to 35 °C and the UV detector set at 284 nm. Liner Sweep Voltammetry (LSV) and electrochemical impedance spectroscopy (EIS) were analyzed on a CHI760E electrochemical workstation to confirm the effect of non-radical reaction in BBC/PS system. The LSV test was measured in 20 mM phosphate buffer (pH = 7) containing PS or 2,4-DCP, while the EIS was taken in 0.1 M KCl containing 5 mM [$Fe(CN)_6^{3-/4-}$]. The electron spin resonance analysis (ESR) was implemented on a Bruker ER200-SRC, which was employed for examining the generated

radicals. 5,5-dimethyl-1-pyrroline N-oxide (DMPO) was chosen as a trapping agent to identify radicals. The $SO_4^{\bullet-}$ and $^{\bullet}OH$ were detected in deionized water and $O_2^{\bullet-}$ was detected in methanol circumstance.

3. Results and discussion

3.1 Morphological characterization

The morphological characterization of BBC was revealed by SEM (Fig. 1, a-b). It is obviously that the BBC has different size of aperture and layered structure. The surface element composition was detected by SEM equipped with EDX (Fig. 1, c-f). The result showed that BBC containing carbon, oxygen, phosphorus and calcium, moreover, the weight percent of these elements are 81.49%, 14.85%, 2.42% and 1.24% respectively (Fig. S1). The phosphorus and calcium were the residue of hydroxyl apatite and all elements evenly distributed throughout BBC.

The information given by nitrogen adsorption/desorption data attested the possession of hierarchical porous carbon in BBC. As shown in Fig. 2a, the distinct typical IV hysteretic loop reveal the existing of slit pores, and the scale of pore distribution is large (density functional theory (DFT) model was applied). It is widely accepted that the coexistence of different aperture can not only shorten the distance of electron transfer but also diminish the resistance [36]. The BBC possesses a myriad of micropores, which might be biggest contribution to the high surface area (1024.34 m^2/g). The high surface area and large range of pore distribution not only enhance the pollutant adsorption, but also facilitate the electron transfer process [37], which is conducive to non-radical reactions.

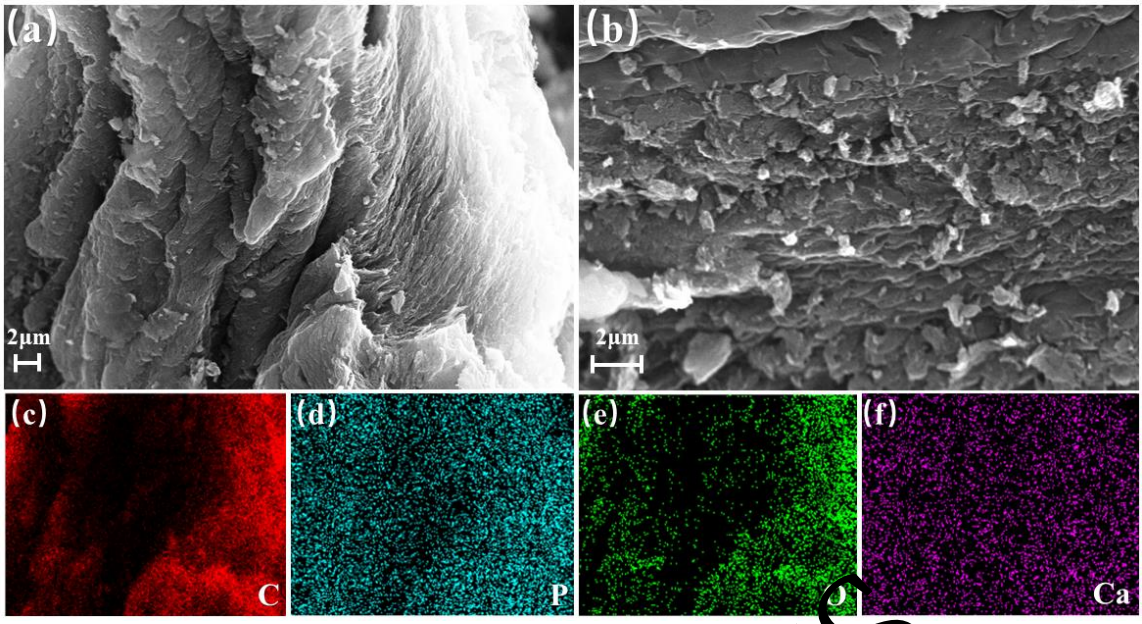

Fig. 1 SEM images (a-b) of BBC in different scale, and corresponding elements mappings of C, O, P and Ca (c-f).

Cursory structure of BBC was explored by the Raman spectrum (Fig. 2b). Peaks occurred at 1350 cm^{-1} and 1580 cm^{-1} are ascribed to the defects and graphite structure respectively. The intensity ratio of these two peaks (I_D/I_G) represent the disorder degree of carbon materials, and the I_D/I_G of BBC is 0.928. It has reported that pyrolysis process could bring defective edges to the biochar boundaries, which terminated with functional group containing oxygen or hydrogen [38, 39]. The appearance of 2D around 2700 cm^{-1} indicates the characteristic of few layers graphite structure, which was in line with the information presented in Fig. 1a and Fig. 2a.

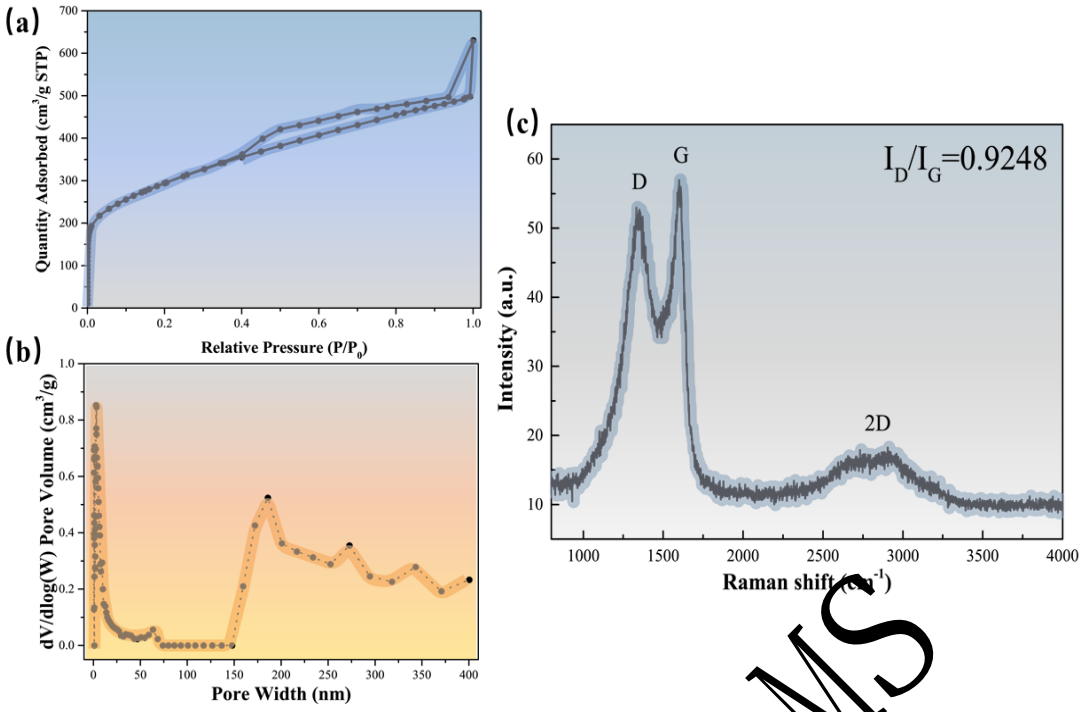

Fig. 2 (a) The nitrogen adsorption/desorption isotherms of BBC, (b) the corresponding pore distribution curve of BBC; (c) the Raman spectra of BBC.

3.2 Catalytic performances

For investigating the contribution of adsorption in BBC/PS system, a 1 h adsorption process was designed. According to the experimental data, 0.2 g/L BBC could adsorb 35% of 2, 4-DCP (0.2 g/L) in 1 h (Fig. 3). The adsorption could achieve by both physics and chemistry process. To be specific, the adsorption capacity might owe to the high surface area and the surface functional groups. Furthermore, when the 2, 4-DCP solution mixed up with PS (2 g/L) without BBC, the concentration only decreased 7% after 2 h reaction.

The effect of the PS dosage was presented in Fig. 3a. The change of PS dosage has little influence on the degradation when the BBC dosage was controlled at 0.2 g/L. Specifically, after 2 h catalysis reaction, the 2, 4-DCP could be removed from 95% to 100% (below the detection limit) when the PS dosage climbed from 0.25 to 4 g/L. However, with the increase of BBC dosage, the reaction rate sharply enhanced. The 2, 4-DCP could

be totally wiped off in 90 min when the BBC increased to 0.5 g/L. Besides, comparing with our published research, BBC could realize similar degradation efficiency with CMK-3 [40]. However, BBC is more economical and environment friendly. Considering that the sulfate ions would bring corrosion problem to pipeline in urban water system [41], and the skyrocketing cost caused by overloading PS. PS dosage should be controlled at a relatively low level. Although 2 g/L PS was used in this study, it is worth noting that in order to save PS input cost in practical applications, even if the PS dosage was reduced to 0.5 g/L, the same removal effect can be achieved but with relatively low reaction rate.

For further understanding of the kinetics of this catalytic reaction, the degradation curve was fitted by the Langmuir-Hinshelwood model of pseudo-first-order kinetics based. The results presented high regression coefficients. It meant that the reaction taken in this system is the first order. k_{obs} was defined as the pseudo-first-order rate constant, and it was acquired by linear regression of Eq. (1).

$$\ln\left(\frac{C_t}{C_0}\right) = -k_{obs}t \quad (1)$$

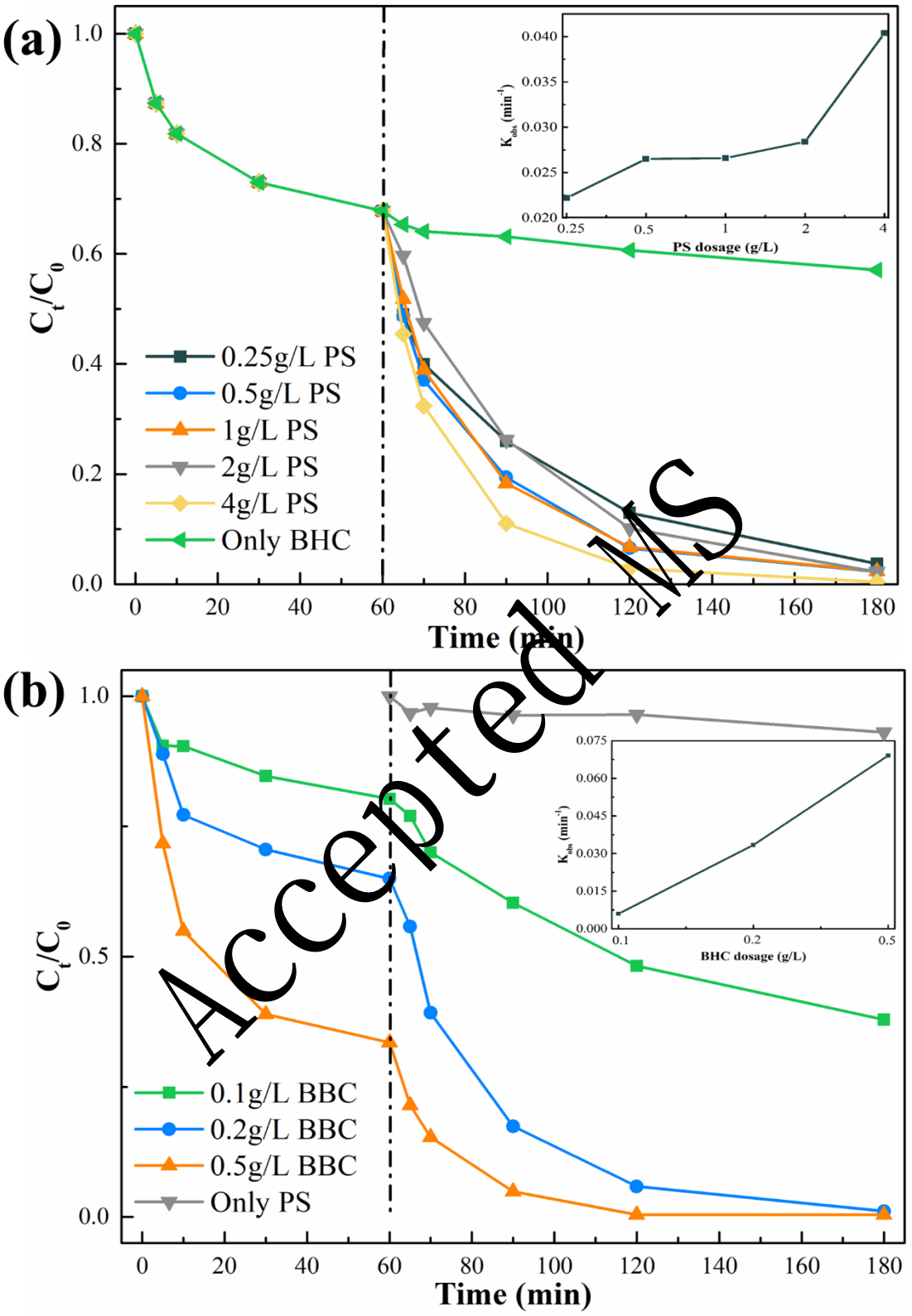

Fig. 3 The influence of (a) PS dosage and (b) BBC dosage on 2, 4-DCP degradation, the insert showed corresponding change of pseudo-first-order rate constant. (the PS concentration was controlled at 2 g/L, the BBC concentration was controlled at 0.2 g/L)

Experimental conditions: [2, 4-DCP] = 0.2 g/L, [Temp] =298 K.

The information given by Fig. 3b illuminating that the k_{obs} soared from 0.006 to 0.0691 min^{-1} when the BBC dosage raised from 0.1 to 0.5 g/L. Previous reports showed that the active sites (oxygenic groups, defect structure, etc.) played an important role in PS activation system [42, 43]. In BBC/PS system, the increase of active sites provided by BBC was accompanied by the soar of reaction rate, which further verified this conclusion. In Fig. 3a, within the change range of PS dosage, the k_{obs} was relative stable and it finally increased to 0.0404 min^{-1} when 4 g/L of PS was added. To address the dechlorination process of 2,4-DCP in BBC/PS system, GC-MS was applied. As shown in Fig. S2, 2,4-DCP dechlorinated through three pathways. The emerged intermediate products (such as phenol, benzoquinone, chlorohydroquinone, et al.) helped to illustrate this conclusion. Besides, the degradation of 2,4-DCP was further verified.

Reaction temperature and pH were further investigated as the effect factors (Fig. 4). For the aim of emphasizing the function of temperature condition in chemical process, the concentration changes of 2, 4-DCP in 2-hour-catalysis at different temperatures were recorded. The reaction rate increased steadily with temperature. Furthermore, without adjustment, the initial pH of 0.2 g/L 2, 4-DCP was 5.15, and the pH was declined to 2.81 after 2 h activation. The impact of different solution initial pH was from 3 to 9 (2, 4-DCP, pK_a=7.85). The experiment results expressed that BBC/PS system exhibited great adaptability within the initial pH adjustment range. However, the optimum initial pH of this system is weak acidic condition.

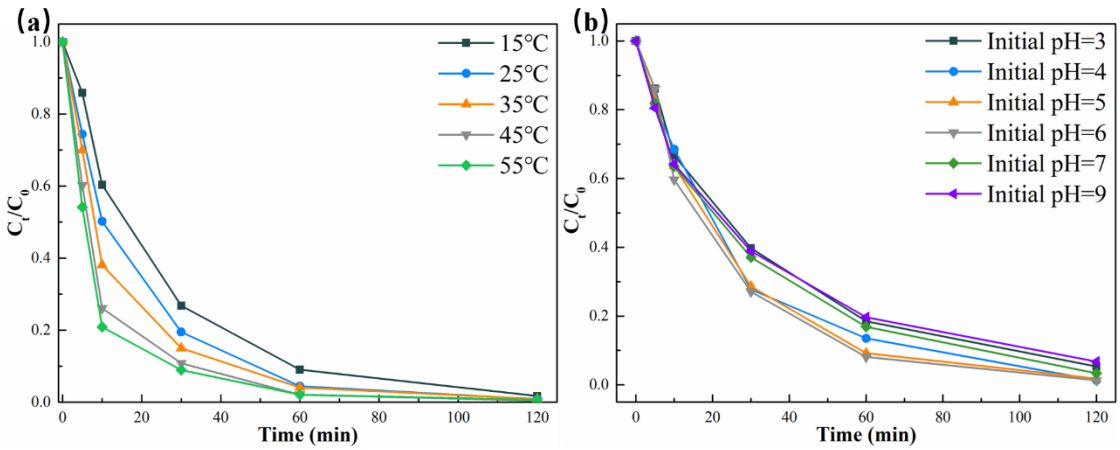

Fig. 4 (a) The effect of temperature on the 2, 4-DCP degradation; (b) The effect of initial pH on the 2, 4-DCP degradation. [2, 4-DCP] = 0.2 g/L, [PS] =2 g/L, [BBC]=0.2 g/L.

3.3 Stability tests

Stability is an important characteristic to catalysis. The stability test can give information about the mechanism of this system. Four cycles were taken to investigate the stability of BBC (Fig. S3). The reaction efficient of 2, 4-DCP sharply decreased to 70% in the 2nd run, and the removal rate further reduced to 45% in 4th run. At the same time, the k_{obs} acutely declined from 0.0334 to 0.0031 min^{-1}. Notably, 1 h adsorption could steadily wipe off 20% of 2, 4-DCP after 1st run and no obvious difference could be seen between 3rd run and 4th run. Consequently, we proposed that there might be a route could operate steadily and not affect by the change on BBC surface [29]. The relatively weak stability may owe to following two reasons: 1) porous was blocked after adsorption process; 2) the inactivation of active site after 1st run.

The variation of BBC surface could be reflected by the XPS survey (Fig. 5b). Comparing with initial BBC, the amount of O in reacted BBC increased from 11.63% to 17.51%. In addition, the existence of Cl on BBC after activation was verified by the peaks located at 200 eV and 270 eV, it is a strong evidence of the dechlorination of 2, 4-DCP.

Additionally, XPS and FTIR have been used for revealing the surface change of BBC before and after reaction. As for the FTIR spectra of BBC, bands centered at 3421, 2372, 1643, 1388 and 1070 cm^{-1} could be observed from Fig. 5a. The bands at 3421 cm^{-1} and 2372 cm^{-1} were characteristics stretching of O-H and -CH_2. The band at 1643 cm^{-1} was assigned to C=O, and the vibration of C=C could be recognized at 1388 cm^{-1}, the band at 1070 cm^{-1} was identified as the characteristic vibration of C-O. After reaction, the band representing the vibration of C=C visibly cut down, while the vibration of C=O (the band at 1643 cm^{-1}) strengthened. It might owe to the change of their relative amount. For verification, XPS high resolution scan of BBC was taken.

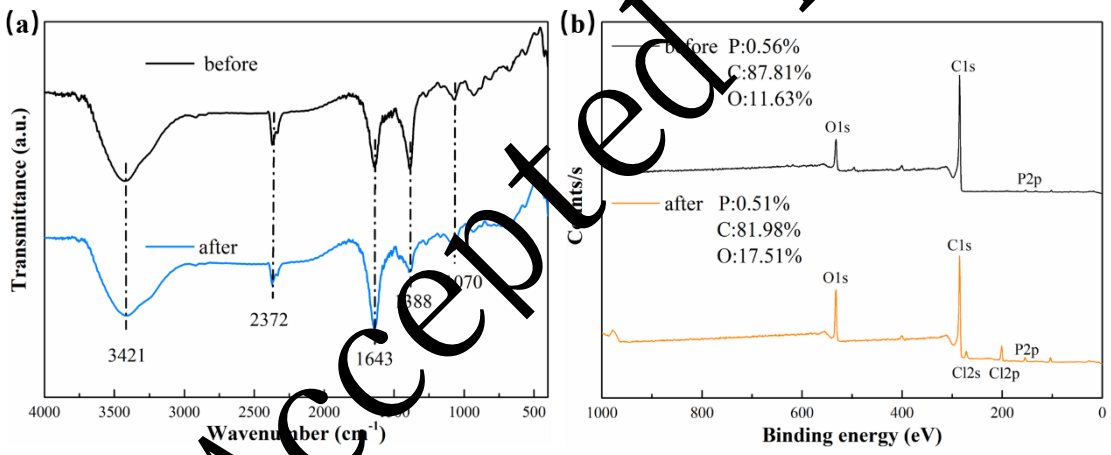

Fig. 5 (a) FTIR spectra and (b) XPS survey of BBC before and after activation.

Fig.6 manifested the specific change of different functional groups. Before reaction, the original peak of C1s could be fitted into four species of 284.85, 285.63, 286.69 and 289.32 eV, representing the stretching vibration of C (graphite), C-OH/C-O-C, C=O and π-π^* shake up respectively. Apparently, the decrease of C-OH/C-O-C was accompanied by the increase of C=O and the appearance of COOH, which reflected the transformation of surface functional groups of BBC. While the extension of C=O could directly lead to the enhancement of the band at 1643 cm^{-1}, the appearance of COOH could be also

reflected by the changes of peak 3421 cm^{-1} and 1643 cm^{-1} in Fig. 5a. The O1s could be divided into three part, while 532.25, 531.06 and 533.10 eV were assigned to the vibration of O_2/H_2O, C-O and C=O, and the change of O1s was in line with that of C1s. Taken the stability tests into account, the surface oxygen-containing functional groups might serve as active sites in BBC/PS system. The decline of removal efficient after first run may be the result of the surface oxidation on BBC.

For a more intuitive validation, phosphorus content remained at the same low level before and after reaction. The high-resolution scan of P2p was displayed in Fig. S4. The peaks at 132.30 eV and 134.01 eV represented C_3-P=O and C-O-P respectively. Whereas, the composition of phosphorus has little change before and after reaction. Although doping heteroatoms (including N, B, O, P, S, etc.) is a common strategy to enhance the efficiency in PS activated reaction for heterogeneous catalytic material [21, 44], the information given by XPS proved that phosphorus doping had no role in BBC/PS system.

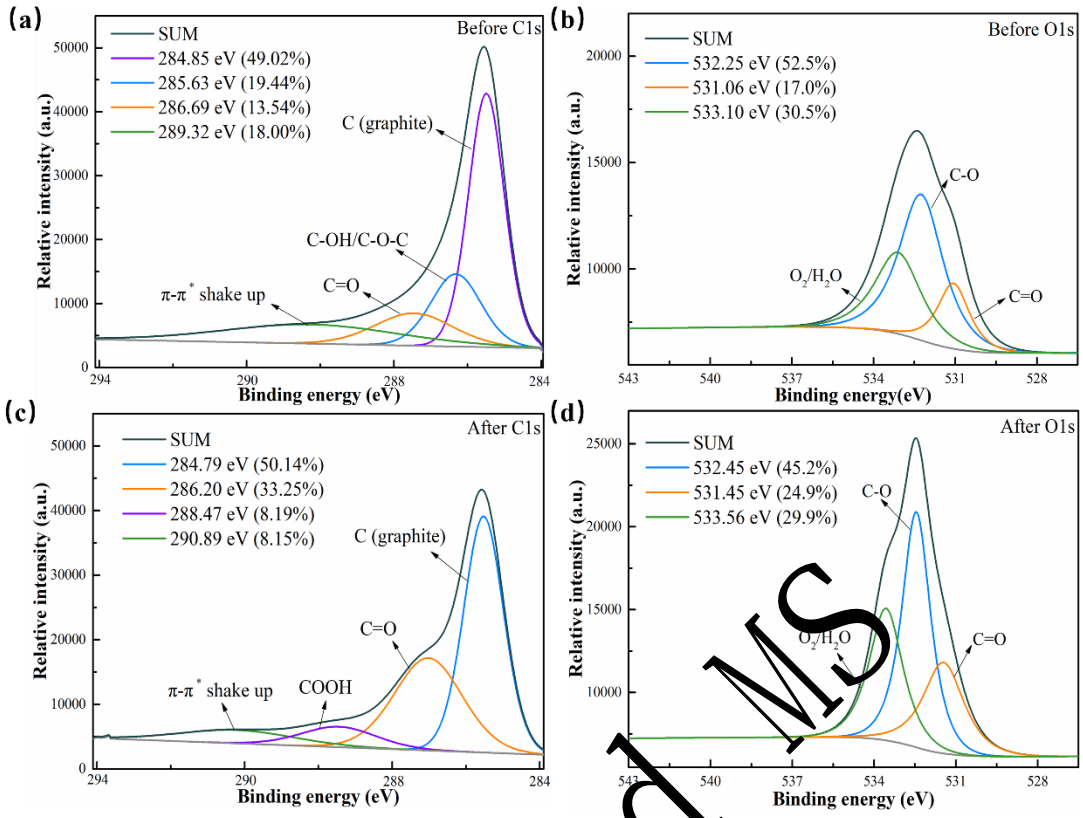

Fig. 6 (a) C1s and (b) O1s spectrums of BBC before reaction; (c) C1s and (d) O1s spectrums of BBC after reaction

To sum up, PS activation was associated with a large-scale variation of functional groups. Studies have declared that surface oxidation plays a significance role in PS activation and both radical and non-radical process contribute to this result [19, 42]. Instead of C=O, C-O were more likely work as active site in BBC/PS system. As electron-rich groups, C-O might act as electron donor in the dechlorination process of 2,4-DCP. Besides, active sites could also promote radical pathway by activating PS to generate radicals. For instance, functional groups on BBC surface ($BBC_{surface}$-COH) could activate PS to generate $SO_4^{\bullet-}$ (Eqs. (2)) [45]

$$BBC_{surface}\text{-}COH + S_2O_8^{2-} \rightarrow BBC_{surface}\text{-}CO\bullet + SO_4^{\bullet-} + HSO_4^- \quad (2)$$

3.4 Free radical pathway

In order to investigate the role of radicals played in this system, the experiment about radical identification have been taken. Free radical is a common process in PS activation [46, 47]. For the aim of lucubrating the degradation mechanism in BBC/PS system, it's necessary to confirm the radicals generated in this system.

Herein, radical quenching reaction have been taken to investigate the effect of different radicals. $^{\bullet}OH$ and $SO_4^{\bullet-}$ were the most common radicals for organic pollutant oxidation in PS activation. Hence, tert-butyl-alcohol (TBA) and ethanol (EtOH) were applied to distinguish the contribution of $^{\bullet}OH$ and $SO_4^{\bullet-}$ for their different reaction rate with two radicals. Generally, EtOH is an effective quencher for both $^{\bullet}OH$ ($k_{^{\bullet}OH}$ = (1.2-2.8) × 10^7 M^{-1} s^{-1}) and $SO_4^{\bullet-}$ ($k_{so4^{\bullet-}}$ = (1.6-7.8) × 10^7 M^{-1} s^{-1}), whereas TBA is effective for $^{\bullet}OH$ ($k_{^{\bullet}OH}$ = (3.8-7.6) × 10^8 M^{-1} s^{-1}) and also poses a relative low impact on $SO_4^{\bullet-}$($k_{so4^{\bullet-}}$ = 4 × 10^5 M^{-1} s^{-1}). Additionally, 1,4-benzoquinone (BQ) was chosen to analyze the effect of superoxide anion radical ($O_2^{\bullet-}$) because the reaction rate constant could up to 1 × 10^9 M^{-1} s^{-1}. Also, studies have clarified that $^1O_2$ might exist in PS activation process [48, 49], so sodium azide (NaN_3) was employed to determine the existence of $^1O_2$ (k=1.2 × 10^8 M^{-1} s^{-1}). When the certain trapping agent was added, the inhibition extent can reflect the corresponding radical amount in this system.

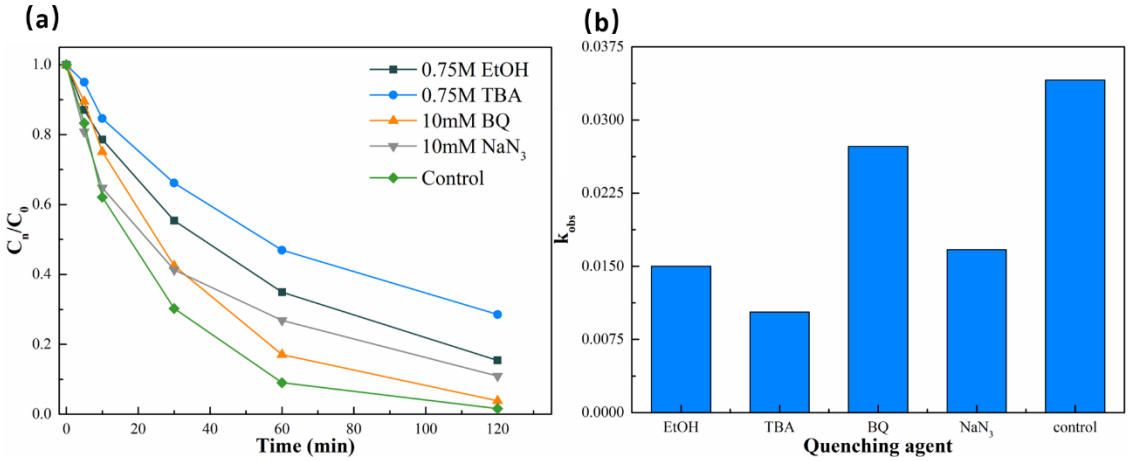

Fig. 7 (a) Effect of EtOH (0.75 M), TBA (0.75 M), BQ (10 mM) and NaN_3 (10 mM) on 2, 4-DCP degradation in BBC/PS system; (b) is the corresponding pseudo-first-order rate constant of different quenching agent. [2, 4-DCP] = 0.2 g/L, [PS] = 2 g/L, [BBC] = 0.2 g/L, [Temp] = 298 K.

Fig. 7 presented the 2 h activation process for each radical quenching batch (C_0 was the concentration of 2,4-DCP after 1 h adsorption). It is obvious that the addition of TBA sharply hindered the reaction, the k_{obs} decreased from 0.0341 to 0.0103 min^{-1}. The inhibitory effect of EtOH was comparatively less than TBA, which manifested that the $^{\cdot}OH$ is the primary radical in BBC/PS system. BQ and NaN_3 can slightly alleviate the reaction rate, and k_{obs} decreased to 0.0273 and 0.0167 min^{-1} respectively. Although excess quencher has been put into, the removal rate of 2, 4-DCP could still reach 72%.

Even though each trapping agent has a distinct trapping effect, simply addition could not quantitatively study the role radical pathway played in BBC/PS system. However, obvious inhibitory effects of each quenching agent might be considered as the favorable evidence for the dominance of radical pathway in this system.

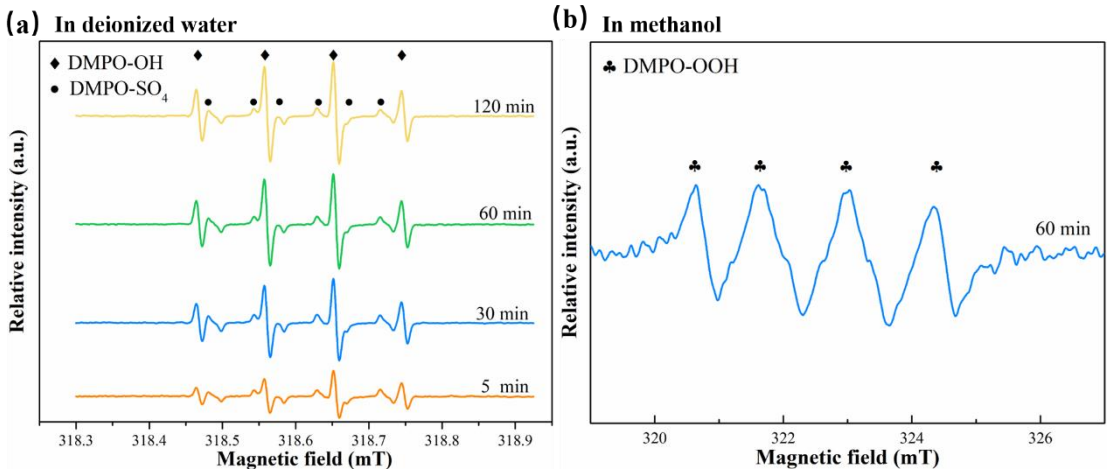

Fig. 8 Electron spin resonance analysis in BBC/PS system (5,5-dimethyl-1-pyrroline N-oxide was the trapping agent). [2, 4-DCP] = 0.2 g/L, [PS] = 2 g/L, [BBC] = 0.2 g/L, [Temp] = 298 K.

The existence of radicals was further determined by ESR spectroscopy, DMPO was applied as the trapping agent. The concentration of ·OH in the system rose gradually during the activation, as the signal peak of ·OH increased with time. The ESR analysis taken in deionized water also manifested that the ·OH played an important role in BBC/PS system, and the $SO_4^{\cdot-}$ did exist in the system but its concentration kept at a low level. Four characteristic peaks in neutral circumstance were recognized for confirming the existence of $O_2^{\cdot-}$. To sum up, ·OH, $SO_4^{\cdot-}$, $O_2^{\cdot-}$ and $^1O_2$ all made sense in BBC/PS system, among which the contribution of ·OH occupied the main position.

3.5 Non-radical pathway

Previous studies unveiled that the non-radical pathway may bring a better selectivity to the target pollutant in complicated environment [19]. Non-radical pathway can degrade pollutants without generating radicals. According to Huang and co-workers, nature porous structure of swine bone derived char worked in electric double-layer capacitors

system. To be specific, macropores could minimize the diffusion distances of ions, mesoporous provide low-resistant pathways, and micropores strengthen the electric double layer capacitance [36]. The ions transfer in the double-layer capacitor was thought to be similar to the electron transfer mechanism of the non-free radical pathway in the PS activation system. So, BBC/PS system is supposed to degrade pollutants by non-radical pathway for its wide porous distribution. The non-radical pathway might work by the electron transferring from PS to 2,4-DCP. Thus, 2,4-DCP might be the electron donor, while PS was the electron acceptor and BBC might act as mediator. It required BBC to be electrically conductive. The formation of pollutant-material-PS ternary construction was deemed as the key to realize the pollutant degradation by electron transfer.

EIS Nyquist plot as an auxiliary characterization was employed as an evidence of the non-radical pathway. According to the electron transfer kinetics at the electrode interface, the semicircle diameter reflects the transfer resistance and the diffusion process is embodied by the straight line [50]. Bare GCE presented a large semicircle diameter in the EIS plots, representing the high resistance. A remarkable decrease of the modified electrode resistance could be observed when the BBC was decorated (Fig. 9a), which indicates a good electron transfer capacity of BBC. The LSV was taken to assess the electron transfer capacity in the corresponding system. As shown in Fig. 9b, when bare glassy carbon electrode (GCE) was used as the work electrode, there almost no current response in 20 mM PBS with PS and 2, 4-DCP. After ornamenting by BBC, there was a minor increase in the presence of PS or 2, 4-DCP, and the obvious peak current value obtained only when PS and 2, 4-DCP were added at the same time. This evidence added

to the theory that the ternary system (BBC, PS and 2, 4-DCP) could accelerate the electron transfer process [40].

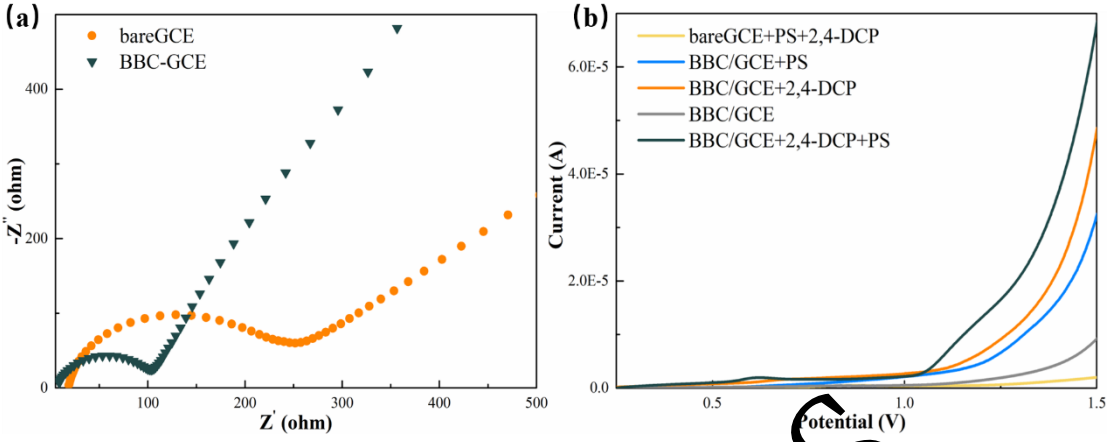

Fig. 9 (a) EIS Nyquist plots of bare GCE and BBC/GCE with frequency range from 0.01 Hz to 10^5 Hz, (b) Linear sweep voltammograms (LSV) obtained by the bare GCE and BBC GCE in the presence of PS or 2, 4-DCP. [2, 4-DCP] = 0.2 g/L, [PS] = 2 g/L, [Temp] = 298 K.

3.6 Real water application

In order to investigate the applicability of BBC/PS system in real water, experiments were taken in real surface water. The surface water was obtained from Xiangjiang River and Taozi Lake (Table 1). Xiangjiang River is the most important river system in Hunan province, it originates in Guangxi province and flows into the Yangtze river system through Dongting Lake. It's an irreplaceable source of drinking water in Hunan. Taozi Lake originates from Yuelu Mountain, it accommodates part of the surrounding sewage. Overall, the BBC/PS system conducted well in real surface water. However, a slight abatement of removal efficiency still existed in both Xiangjiang River and Taozi Lake, and the inhibition in Taozi Lake was more apparent. The hypothesis that the organics in the real water samples may have competitive adsorption effect to 2, 4-DCP was proposed.

In order to verify this assumption, the chemical oxygen demand (COD, a chemical indicator which can describe the organic amount of surface water) value was obtained by the method specified in the Chinese national standard. The COD of Xiangjiang River is 8.0 mg/L, while that of Taozi Lake is 13.1 mg/L.

Table 1 Sampling information of different water samples

Location	Sampling site	Chemical oxygen demand (COD)
Taozi Lake	E 112.95°, N 28.18°	13.1 mg/L
Xiangjiang River	E 112.59°, N 28.17°	8.0 mg/L

The results showed that the removal rate of 2, 4-DCP was declined with the increasing of COD. The decrease in the degree of degradation may be due to the competition between the organic matter in the surface water and the target pollutant for the active sites of the BBC. This phenomenon was tally with the hypothesis put forward beforehand.

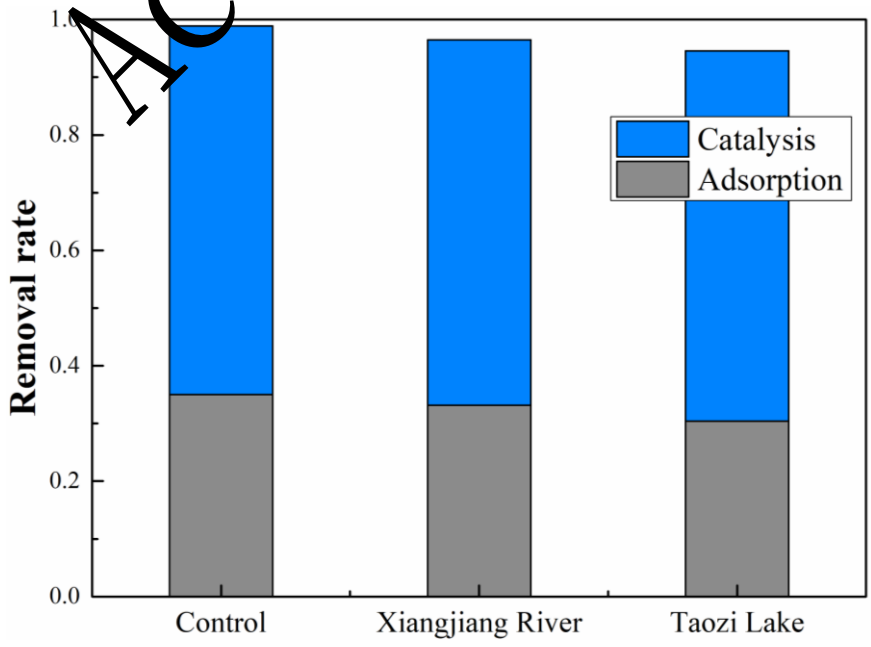

Fig. 10 BBC/PS system utilized in real surface water to degrade 2, 4-DCP, [2, 4-DCP] = 0.2 g/L, [PS] = 2 g/L, [BBC] = 0.2 g/L, [Temp] = 298 K.

Cl^- is widely spread in wastewater and it may serve as a capture reagent of radicals [40, 51]. Consequently, it is necessary to investigate the influence of Cl^- on BBC/PS system. As seen from Fig. S5, there was a little inhibition of reaction rate when 5 mM Cl^- was added, and the inhibitory effect increased with the concentration of Cl^- within limits. This phenomenon may because a handful of Cl^- could act as scavengers of $^{\bullet}OH$ and $SO_4^{\bullet-}$. According to the radical reaction mechanism, the Cl^- could combine with $^{\bullet}OH$ and $SO_4^{\bullet-}$ to form $Cl^{\bullet}$ (2.4 eV) and $Cl_2^{\bullet-}$ (2.1 eV) for their redox potential were lower than $^{\bullet}OH$ and $SO_4^{\bullet-}$ (Eqs. (3)-(6)). It may be the reason of the inhibition at low Cl^- concentration. However, the inhibition effect was alleviated at the end of the reaction when 10 mM and 20 mM Cl^- was added. It may be because that with the dechlorination of 2, 4-DCP, the concentration of Cl^- in the solution increased to an excessive level. Additionally, while the concentration of Cl^- raised to 100 mM, a promotion of 2, 4-DCP removal rate could be distinguished. This phenomenon occurred might because the superfluous Cl^- could serve as electron donor to accelerate the reaction [40]. Wang's group first reported that superabundant Cl^- could activate PS without catalytic material, and it can be regarded as non-radical pathway to some extent [52]. Our group have reported that the acceleration could be seen when 20 mM Cl^- was added [40]. And in cobalt ion activation system, reaction can only promote when coexisting with over 500 mM Cl^- [52]. Further comparing with this experiment, the distribution of non-radical and radical pathway may be the reason for different critical point of the influence of Cl^-. So, the assumption that

Cl^- could accelerate the reaction through non-radical pathway and alleviate the process through radical pathway was proposed. The ultimate impact in certain system is up to the different proportion of radical and non-radical pathway.

$$SO_4^{\bullet-} + Cl^- \rightarrow Cl^{\bullet} + SO_4^{2-} \quad (3)$$

$$^{\bullet}OH + Cl^- \rightarrow ClOH^{\bullet-} \quad (4)$$

$$ClOH^{\bullet-} + Cl^- \rightarrow Cl_2^{\bullet-} + OH^- \quad (5)$$

$$Cl^{\bullet} + Cl^- \rightarrow Cl_2^{\bullet-} \quad (6)$$

3.7 Antibiotic degradation

Antibiotic recently got much attention of researchers and gradually became the urgent contaminant in environment [53-57]. In order to investigate the adaptability of BBC/PS system, BBC/PS system was also devoted to degrading antibiotic (Fig. S6). Tetracycline (TC) and sulfamethoxazole (SMX) were chosen as the typical antibiotic in environment. The results declared that this system also performed well on antibiotic degradation, and a higher adsorption capacity was shown when antibiotic was chosen as the target pollutant. The increasing of adsorption capacity might owe to the formation of hydrogen bonding between antibiotics and BBC. Conclusion could be made that the BBC/PS system had the ability to degrade different pollutants with diverse structure in aqueous environment.

3.8 Multiple mechanism system

Take all the experimental results into consideration, the assumption that the BBC/PS system achieved an effective degradation through both radical and non-radical pathways was tested. Excellent characteristics of BBC is the key in this system. Hierarchical porous

structure of BBC could not only enhance the adsorption capacity but also accelerate electron transfer process. Moreover, the electron-rich group on BBC could promote both radical and non-radical pathway by assisting the generation of radicals and donating electron.

As for non-radical process, BBC was pivotal, since it was deemed as a mediator to facilitate the transfer of electrons from 2, 4-DCP to PS or H_2O (Eq. (7)). Firstly, the non-radical process relied on the adsorption capacity of BBC. Only after the tight bond of BBC, PS and 2,4-DCP, the electron transfer could be achieved. Moreover, the hierarchical porous structure helped PS and 2,4-DCP molecules get inside the BBC to enhance the pore utilization. Secondly, comparing with other carbonaceous materials, hierarchical porous carbon such as BBC might promote the electron transfer process. As mentioned above, macropores could minimize the diffusion distances of electron, mesoporous provide low-resistant pathways, and micropores might promote non-radical pathway by enhancing the adsorption capacity of the materials.

Besides, radical pathway played a crucial role in BBC/PS system. $^{\bullet}OH$, $SO_4^{\bullet-}$, $O_2^{\bullet-}$ and $^1O_2$ were all participated in PS activation (Eqs. (8)-(12)). In section 3.3, the function of oxygenic groups on BBC surface has been manifested. The adsorption of PS is the prerequisite of radicals' generation. Thus, the porous structure not only is the key factor of non-radical pathway but also can assist radical pathway. At the beginning of the radical reaction, BBC promoted the reaction between $S_2O_8^{2-}$ and H_2O to generate $SO_4^{\bullet-}$ and $O_2^{\bullet-}$. In the presence of OH^-, the $SO_4^{\bullet-}$ could convert OH^- into $^{\bullet}OH$. As mentioned above, $^{\bullet}OH$ is the main ones among various radicals in this system. Although $^{\bullet}OH$ might prefer to

generate at alkaline condition, the optimum initial pH of this system was at weak acidic condition. It might be the result of the radicals with low activity could not degrade the pollutant. There are many factors influence the activity of radicals, while pH might be an important one. According to previous study, with the increase of pH, the redox potential of ·OH dropped from 2.8 eV to 1.5 eV [58]. Furthermore, the produce of ·OH accompanied with the plentiful consumption of OH^-, this might the reason of the reduction of pH during the 2 h activation process. From the perspective of reactive oxygen species, at the beginning of the activated reaction, the NaN_3 (10 mM) had little effect and the inhibition of BQ (10 mM) was diminished at the end of the reaction (Fig. 7). This might because there is a certain transformation relationship between $O_2^{\bullet-}$ and $^1O_2$ in solution. As the catalytic reaction goes on, excess free ·OH and H^+ could combine with $O_2^{\bullet-}$ to produce $^1O_2$.

$$S_2O_8^{2-} + 2e^- \rightarrow 2SO_4^{2-} \quad (7)$$

$$S_2O_8^{2-} + 2H_2O \rightarrow 2SO_4^{2-} + HO_2^- + H^+ \quad (8)$$

$$S_2O_8^{2-} + HO_2^- \rightarrow 2SO_4^{2-} + SO_4^{\bullet-} + H^+ + O_2^{\bullet-} \quad (9)$$

$$SO_4^{\bullet-} + OH^- \rightarrow {}^{\bullet}OH + SO_4^{2-} \quad (10)$$

$$^{\bullet}OH + O_2^{\bullet-} \rightarrow {}^1O_2 + OH^- \quad (11)$$

$$2H^+ + 2O_2^{\bullet-} \rightarrow {}^1O_2 + H_2O_2 \quad (12)$$

Multiple mechanisms in the system can help it adapt to various conditions. This verdict could be supported by the adaptation of wide range of pH and the less affected by COD and Cl^-. So, BBC/PS system could be considered as a prospective method to widely applied in actual wastewater treatment.

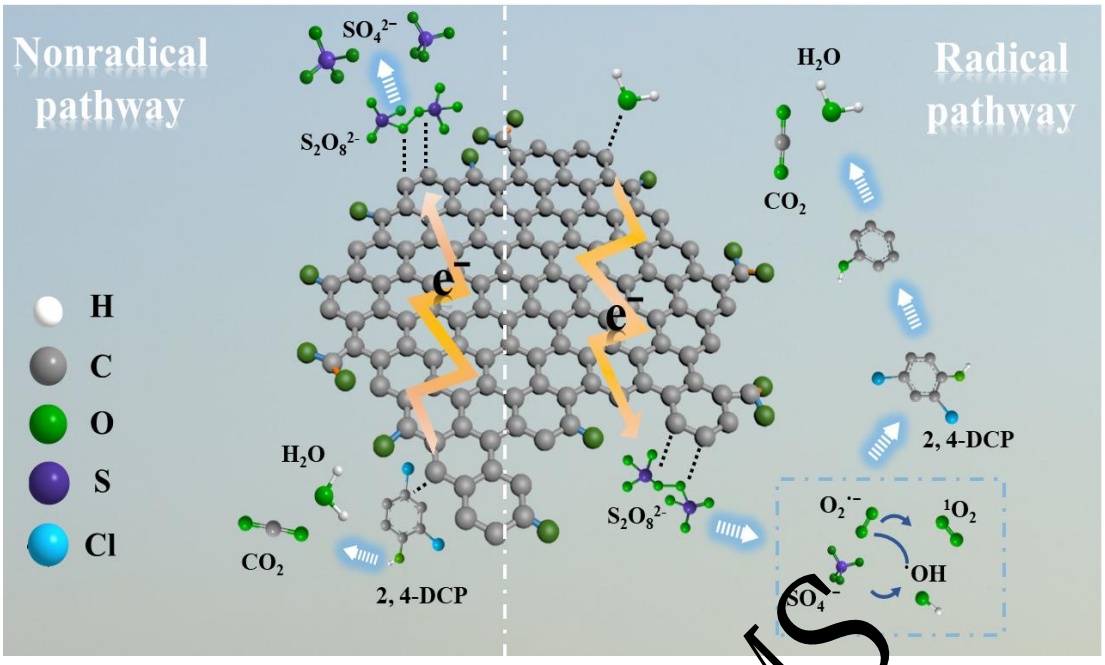

Scheme 1 Proposed mechanism of PS on bone char-derived hierarchical porous carbon

4. Conclusion

To sum up, BBC/PS system could be a promising option for organic pollutant degradation. As a kind of biochar, BBC worked by both adsorption and catalysis. This system degraded the organic by both radical and non-radical pathway, and the radical pathway share a majority proportion of the degradation. Among various radicals existed in this system, $^{\bullet}OH$ play a vital role in the radical reaction. With respect to the effect of ions on this system, since Cl^- can affect radical and non-radical pathway in different ways, adjusting material structure could achieve the best efficiency of practical conditions. The existence of multiple mechanisms enhanced the adaptive capacity of BBC. Moreover, BBC/PS system worked well in a wide pH range, and it also efficiently degraded target pollutant in real surface water. The application of the bone carbon provides a new strategy for high efficiency green remediation of organic contaminants.

Acknowledgements

This study was financially supported by the Program for the National Natural Science Foundation of China (51879101, 51579098, 51779090, 51709101, 51521006, 51809090, 51278176, 51378190), the National Program for Support of Top–Notch Young Professionals of China (2014), the Program for Changjiang Scholars and Innovative Research Team in University (IRT-13R17), and Hunan Provincial Science and Technology Plan Project (2018SK20410, 2017SK2243, 2016RS3026), and the Fundamental Research Funds for the Central Universities (531113200086, 531118010114, 531107050978).

Compliance with ethical standards

Conflict of interest: The authors declare that they have no competing interest.

Reference

[1] X. Zhou, C. Lai, D. Huang, G. Zeng, L. Chen, L. Qin, P. Xu, M. Cheng, C. Huang, C. Zhang, Preparation of water-compatible molecularly imprinted thiol-functionalized activated titanium dioxide: Selective adsorption and efficient photodegradation of 2, 4-dinitrophenol in aqueous solution, J. Hazard. Mater. 346 (2018) 113-123.

[2] Z. Huang, K. He, Z. Song, G. Zeng, A. Chen, L. Yuan, H. Li, L. Hu, Z. Guo, G. Chen, Antioxidative response of Phanerochaete chrysosporium against silver nanoparticle-induced toxicity and its potential mechanism, Chemosphere 211 (2018) 573-583.

[3] B. Li, C. Lai, G. Zeng, D. Huang, L. Qin, M. Zhang, M. Cheng, X. Liu, H. Yi, C. Zhou, Black Phosphorus, a Rising Star 2D Nanomaterial in the Post-Graphene Era: Synthesis, Properties, Modifications, and Photocatalysis Applications, Small 15 (2019) 1804565.

[4] H. Yi, M. Yan, D. Huang, G. Zeng, C. Lai, M. Li, X. Huo, L. Qin, S. Liu, X. Liu, Synergistic effect of artificial enzyme and 2D nanostructured Bi2WO6 for eco-friendly and efficient biomimetic photocatalysis, Appl. Catal. B (2019).

[5] C. Lai, M.-M. Wang, G.-M. Zeng, Y.-G. Liu, D.-L. Huang, C. Zhang, R.-Z. Wang, P. Xu, M. Cheng, C. Huang, Synthesis of surface molecular imprinted TiO2/graphene photocatalyst and its highly efficient photocatalytic degradation of target pollutant under visible light irradiation, Appl. Surf. Sci. 390 (2016) 368-376.

[6] Y. Yang, C. Zhang, C. Lai, G. Zeng, D. Huang, M. Cheng, J. Wang, F. Chen, C. Zhou, W. Xiong, BiOX (X= Cl, Br, I) photocatalytic nanomaterials: applications for fuels and environmental management, Adv. Colloid Interface Sci. 254 (2018) 76-93.

[7] C. Zhou, C. Lai, C. Zhang, G. Zeng, D. Huang, M. Cheng, L. Hu, W. Xiong, M. Chen, J. Wang, Semiconductor/boron nitride composites: synthesis, properties, and photocatalysis applications, Appl. Catal. B (2018).

[8] B. Li, C. Lai, P. Xu, G. Zeng, D. Huang, L. Qin, H. Yi, M. Cheng, L. Wang, F. Huang, Facile synthesis of bismuth oxyhalogen-based Z-scheme photocatalyst for visible-light-driven pollutant removal: Kinetics, degradation pathways and mechanism, J. Cleaner Prod. 225 (2019) 898-912.

[9] Y. Zhang, X. Yuan, W. Lu, Y. Yan, J. Zhu, T.-W. Chou, MnO2 based sandwich structure electrode for supercapacitor with large voltage window and high mass loading, Chem. Eng. J. 368 (2019) 525-532.

[10] D. Huang, R. Deng, J. Wan, G. Zeng, W. Xue, X. Wen, C. Zhou, L. Hu, X. Liu, P. Xu, Remediation of lead-contaminated sediment by biochar-supported nano-chlorapatite: Accompanied with the change of available phosphorus and organic matters, J. Hazard. Mater. 348 (2018) 109-116.

[11] L. Li, C. Lai, F. Huang, M. Cheng, G. Zeng, D. Huang, B. Li, S. Liu, M. Zhang, L. Qin, M. Li, J. He, Y. Zhang, L. Chen, Degradation of naphthalene with magnetic bio-char activate hydrogen peroxide: Synergism of bio-char and Fe–Mn binary oxides, Water Res. 160 (2019) 238-248.

[12] A.V. Levanov, O.Y. Isaikina, R.B. Gasanova, A.S. Uzhel, V.V. Lunin, Kinetics of chlorate formation during ozonation of aqueous chloride solutions, Chemosphere 229 (2019) 68-76.

[13] P. Hu, M. Long, Cobalt-catalyzed sulfate radical-based advanced oxidation: A review on heterogeneous catalysts and applications, Appl. Catal. B 181 (2016) 103-117.

[14] X. Duan, C. Su, J. Miao, Y. Zhong, Z. Shao, S. Wang, H. Sun, Insights into perovskite-catalyzed peroxymonosulfate activation: Maneuverable cobalt sites for promoted evolution of sulfate radicals, Appl. Catal. B 220 (2018) 626-634.

[15] H. Lee, H.-J. Lee, J. Jeong, J. Lee, N.-B. Park, C. Lee, Activation of persulfates by carbon nanotubes: Oxidation of organic compounds by nonradical mechanism, Chem. Eng. J.266 (2015) 28-33.

[16] W.-D. Oh, Z. Dong, T.-T. Lim, Generation of sulfate radical through heterogeneous catalysis for organic contaminants removal: Current development, challenges and prospects, Appl. Catal. B 194 (2016) 169-201.

[17] L. Qin, Z. Zeng, G. Zeng, C. Lai, A. Duan, R. Xiao, D. Huang, Y. Fu, H. Yi, B. Li, Cooperative catalytic performance of bimetallic Ni-Au nanocatalyst for highly efficient hydrogenation of nitroaromatics and corresponding mechanism insight, Appl. Catal. B 259 (2019) 118035.

[18] X. Duan, H. Sun, J. Kang, Y. Wang, S. Indrawirawan, S. Wang, Insights into Heterogeneous Catalysis of Persulfate Activation on Dimensional-Structured Nanocarbons, ACS Catal. 5 (2015) 4629-4636.

[19] X. Duan, H. Sun, Z. Shao, S. Wang, Nonradical reactions in environmental remediation processes: Uncertainty and challenges, Applied Catalysis B: Environmental 224 (2018) 973-982.

[20] Y. Fu, L. Qin, D. Huang, G. Zeng, C. Lai, B. Li, J. He, H. Yi, M. Zhang, M. Cheng, Chitosan functionalized activated coke for Au nanoparticles anchoring: Green synthesis and catalytic activities in hydrogenation of nitrophenols and azo dyes, Appl. Catal. B 255 (2019) 117740.

[21] X. Duan, Z. Ao, H. Sun, S. Indrawirawan, Y. Wang, J. Kang, F. Liang, Z.H. Zhu, S. Wang, Nitrogen-doped graphene for generation and evolution of reactive radicals by metal-free catalysis, ACS Appl. Mater. Interfaces 7 (2015) 4169-4178.

[22] G. Millhauser, D. Thompson, K. Bolin, D. Anderson, J. McNulty, Methods and compounds for modulating melanocortin receptor ligand binding and activity, Google Patents, 2003.

[23] K. He, Z. Zeng, A. Chen, G. Zeng, R. Xiao, P. Xu, Z. Huang, J. Shi, L. Hu, G. Chen, Advancement of Ag–graphene based nanocomposites: an overview of synthesis and its applications, Small 14 (2018) 1800871.

[24] X. Duan, Z. Ao, H. Sun, L. Zhou, G. Wang, S. Wang, Insights into N-doping in single-walled carbon nanotubes for enhanced activation of superoxides: a mechanistic study, Chem Commun (Camb) 51 (2015) 15249-15252.

[25] M.J. Olszta, X. Cheng, S.S. Jee, R. Kumar, Y.-Y. Kim, M.J. Kaufman, E.P. Douglas, L.B. Gower, Bone structure and formation: A new perspective, Mat. Sci. Eeg. R 58 (2007) 77-116.

[26] Y. Zhang, Z. Ma, J. Yan, Influence of pork and bone on product characteristics during the fast pyrolysis of pig carcasses, Waste Manag 75 (2018) 352-360.

[27] X. Rong, M. Xie, L.S. Kong, V. Natarajan, L. Ma, J.H. Zhan, The magnetic biochar derived from banana peels as a persulfate activator for organic contaminants degradation,

Chem. Eng. J. 372 (2019) 294-303.

[28] H.Z. Wang, W.Q. Guo, B.H. Liu, Q.L. Wu, H.C. Luo, Q. Zhao, Q.S. Si, F. Sseguya, N.Q. Ren, Edge-nitrogenated biochar for efficient peroxydisulfate activation: An electron transfer mechanism, Water Res. 160 (2019) 405-414.

[29] B.-C. Huang, J. Jiang, G.-X. Huang, H.-Q. Yu, Sludge biochar-based catalysts for improved pollutant degradation by activating peroxymonosulfate, J. Mater. Chem. A 6 (2018) 8978-8985.

[30] Y. Wang, Y. Zhu, Y. Hu, G. Zeng, Y. Zhang, C. Zhang, C. Feng, How to construct DNA hydrogels for environmental applications: advanced water treatment and environmental analysis, Small 14 (2018) 1703305.

[31] R.-Z. Wang, D.-L. Huang, Y.-G. Liu, C. Zhang, C. Lai, X. Wang, G.-M. Zeng, X.-M. Gong, A. Duan, Q. Zhang, Recent advances in biochar-based catalysts: properties, applications and mechanisms for pollution remediation, Chem. Eng. J. (2019).

[32] H. Wang, W. Guo, R. Yin, J. Du, Q. Wu, H. Luo, B. Liu, F. Sseguya, N. Ren, Biochar-induced Fe(III) reduction for persulfate activation in sulfamethoxazole degradation: Insight into the electron transfer, radical oxidation and degradation pathways, Chem. Eng. J. 362 (2019) 561-569.

[33] S.S.A. Alkurdi, I. Herath, J. Bundschuh, R.A. Al-Juboori, M. Vithanage, D. Mohan, Biochar versus bone char for a sustainable inorganic arsenic mitigation in water: What needs to be done in future research?, Environment International 127 (2019) 52-69.

[34] S.S.A. Alkurdi, R.A. Al-Juboori, J. Bundschuh, I. Hamawand, Bone char as a green sorbent for removing health threatening fluoride from drinking water, Environ. Int. 127 (2019) 704-719.

[35] J.-Y. Rho, L. Kuhn-Spearing, P. Zioupos, Mechanical properties and the hierarchical structure of bone, Med. Eng. Phys. 20 (1998) 92-102.

[36] W. Huang, H. Zhang, Y. Huang, W. Wang, S. Wei, Hierarchical porous carbon obtained from animal bone and evaluation in electric double-layer capacitors, Carbon 49 (2011) 838-843.

[37] S. Dutta, A. Bhaumik, K.C.W. Wu, Hierarchically porous carbon derived from

polymers and biomass: effect of interconnected pores on energy applications, Energy Environ. Sci. 7 (2014) 3574-3592.

[38] M. Keiluweit, P.S. Nico, M.G. Johnson, M. Kleber, Dynamic molecular structure of plant biomass-derived black carbon (biochar), Environmental science & technology 44 (2010) 1247-1253.

[39] C. Guizani, K. Haddad, L. Limousy, M. Jeguirim, New insights on the structural evolution of biomass char upon pyrolysis as revealed by the Raman spectroscopy and elemental analysis, Carbon 119 (2017) 519-521.

[40] L. Tang, Y. Liu, J. Wang, G. Zeng, Y. Deng, H. Dong, H. Feng, J. Wang, B. Peng, Enhanced activation process of persulfate by mesoporous carbon for degradation of aqueous organic pollutants: Electron transfer mechanism, Appl. Catal. B 231 (2018) 1-10.

[41] I. Pikaar, K.R. Sharma, S. Hu, W. Gernjak, J. Keller, Z. Yuan, Reducing sewer corrosion through integrated urban water management, Science 345 (2014) 812-814.

[42] X. Duan, Z. Ao, L. Zhou, H. Sun, G. Wang, S. Wang, Occurrence of radical and nonradical pathways from carbocatalysts for aqueous and nonaqueous catalytic oxidation, Appl. Catal. B 188 (2016) 98-105.

[43] P. Liang, C. Zhang, X. Duan, H. Sun, S. Liu, M.O. Tade, S. Wang, An insight into metal organic framework derived N-doped graphene for the oxidative degradation of persistent contaminants: formation mechanism and generation of singlet oxygen from peroxymonosulfate, Environ. Sci. Nano 4 (2017) 315-324.

[44] X. Duan, H. Sun, Y. Wang, J. Kang, S. Wang, N-Doping-Induced Nonradical Reaction on Single-Walled Carbon Nanotubes for Catalytic Phenol Oxidation, ACS Catal. 5 (2014) 553-559.

[45] J. Yan, L. Han, W. Gao, S. Xue, M. Chen, Biochar supported nanoscale zerovalent iron composite used as persulfate activator for removing trichloroethylene, Bioresour Technol 175 (2015) 269-274.

[46] R. Matta, S. Tlili, S. Chiron, S. Barbati, Removal of carbamazepine from urban wastewater by sulfate radical oxidation, Environ. Chem. Lett. 9 (2010) 347-353.

[47] S. Wacławek, H.V. Lutze, K. Grübel, V.V.T. Padil, M. Černík, D.D. Dionysiou, Chemistry of persulfates in water and wastewater treatment: A review, Chem. Eng. J. 330 (2017) 44-62.

[48] S. Zhao, X. Zhao, Insights into the role of singlet oxygen in the photocatalytic hydrogen peroxide production over polyoxometalates-derived metal oxides incorporated into graphitic carbon nitride framework, Appl. Catal. B 250 (2019) 408-418.

[49] S.S. Gill, N. Tuteja, Reactive oxygen species and antioxidant machinery in abiotic stress tolerance in crop plants, Plant Physiol Biochem 48 (2010) 909-930.

[50] C. Lai, S. Liu, C. Zhang, G. Zeng, D. Huang, L. Qin, X. Liu, H. Yi, R. Wang, F. Huang, B. Li, T. Hu, Electrochemical Aptasensor Based on Sulfur–Nitrogen Codoped Ordered Mesoporous Carbon and Thymine–Hg2+–Thymine Mismatch Structure for Hg2+ Detection, ACS Sensors 3 (2018) 2566-2573.

[51] Z. Wang, R. Yuan, Y. Guo, L. Xu, J. Liu, Effects of chloride ions on bleaching of azo dyes by Co2+/oxone reagent: kinetic analysis, J. Hazard. Mater. 190 (2011) 1083-1087.

[52] Z. Wang, R. Yuan, Y. Guo, L. Xu, J. Liu, Effects of chloride ions on bleaching of azo dyes by Co2+/oxone regent: kinetic analysis, J. Hazard. Mater. 190 (2011) 1083-1087.

[53] C. Lai, X. Liu, L. Qin, C. Zhang, G. Zeng, D. Huang, M. Cheng, P. Xu, H. Yi, D. Huang, Chitosan-wrapped gold nanoparticles for hydrogen-bonding recognition and colorimetric determination of the antibiotic kanamycin, Microchimica Acta 184 (2017) 2097-2105.

[54] L. Qin, G. Zeng, C. Lai, D. Huang, C. Zhang, P. Xu, T. Hu, X. Liu, M. Cheng, Y. Liu, A visual application of gold nanoparticles: simple, reliable and sensitive detection of kanamycin based on hydrogen-bonding recognition, Sens. Actuator B 243 (2017) 946-954.

[55] C. Lai, M. Zhang, B. Li, D. Huang, G. Zeng, L. Qin, X. Liu, H. Yi, M. Cheng, L. Li, Fabrication of CuS/BiVO4 (0 4 0) binary heterojunction photocatalysts with enhanced photocatalytic activity for Ciprofloxacin degradation and mechanism insight, Chemical Engineering Journal 358 (2019) 891-902.

[56] D. Huang, X. Wang, C. Zhang, G. Zeng, Z. Peng, J. Zhou, M. Cheng, R. Wang, Z.

Hu, X. Qin, Sorptive removal of ionizable antibiotic sulfamethazine from aqueous solution by graphene oxide-coated biochar nanocomposites: influencing factors and mechanism, Chemosphere 186 (2017) 414-421.

[57] M. Zhang, C. Lai, B. Li, D. Huang, G. Zeng, P. Xu, L. Qin, S. Liu, X. Liu, H. Yi, Rational design 2D/2D BiOBr/CDs/g-C3N4 Z-scheme heterojunction photocatalyst with carbon dots as solid-state electron mediators for enhanced visible and NIR photocatalytic activity: Kinetics, intermediates, and mechanism insight, Chin. J. Catal. Chinese 369 (2019) 469-481.

[58] C. Lai, F. Huang, G. Zeng, D. Huang, L. Qin, M. Cheng, C. Zhang, B. Li, H. Yi, S. Liu, L. Li, L. Chen, Fabrication of novel magnetic MnFe2O4/bio-char composite and heterogeneous photo-Fenton degradation of tetracycline in near neutral pH, Chemosphere 224 (2019) 910-921.